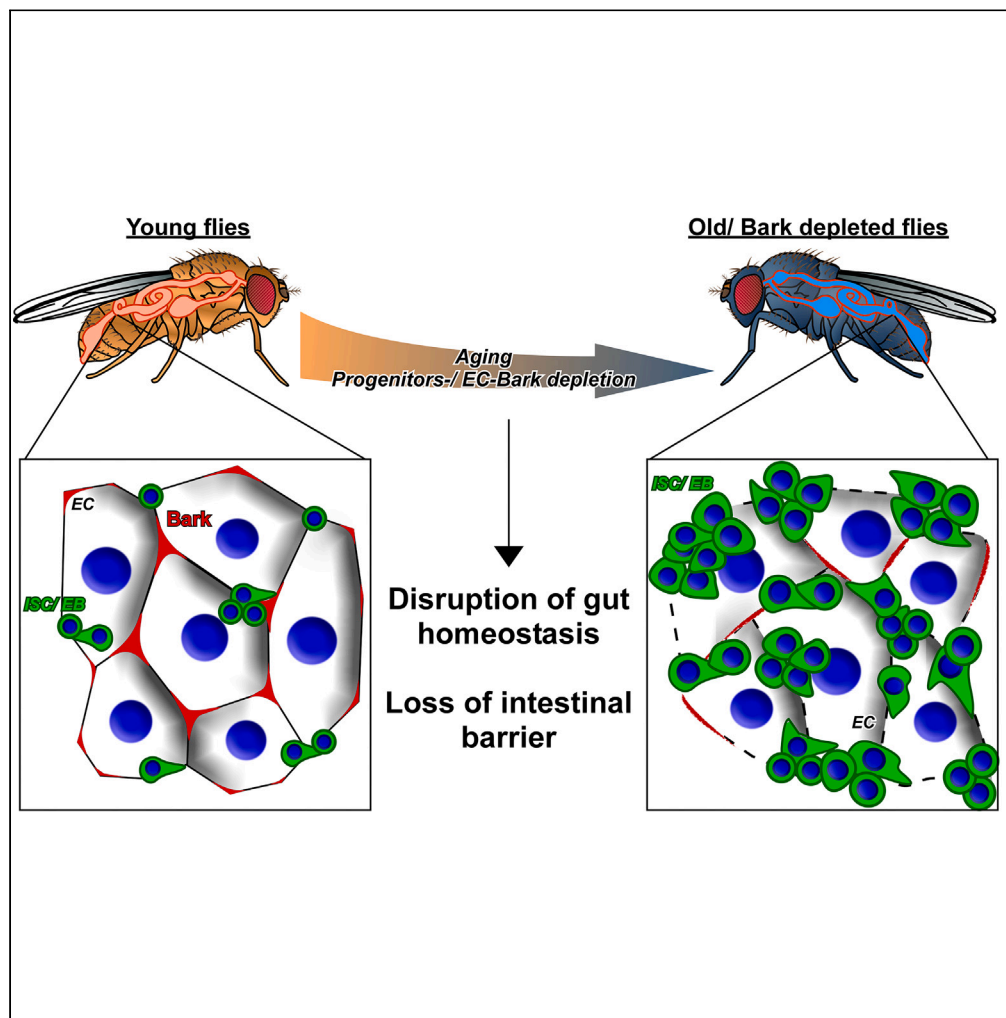**Article**

The septate junction component bark beetle is required for *Drosophila* intestinal barrier function and homeostasis

Rachel A. Hodge, Mirna Ghannam, Emma Edmond, ..., Martin Resnik-Docampo, Tobias Reiff, D. Leanne Jones

leanne.jones@ucsf.edu

Highlights

Bark is lost from the tricellular junction in ECs of old flies

Bark is required in enterocytes (ECs) to maintain intestinal homeostasis

Bark is required in enteroblasts (EBs) for proper differentiation of progenitor cells

Loss of bark may contribute to age-related loss of intestinal homeostasis

Article

The septate junction component bark beetle is required for *Drosophila* intestinal barrier function and homeostasis

Rachel A. Hodge,[1] Mirna Ghannam,[2] Emma Edmond,[1] Fernando de la Torre,[1] Cecilia D'Alterio,[1] Nida Hatice Kaya,[2] Martin Resnik-Docampo,[1] Tobias Reiff,[2] and D. Leanne Jones[1,3,4,5,6,7,*]

SUMMARY

Age-related loss of intestinal barrier function has been documented across species, but the causes remain unknown. The intestinal barrier is maintained by tight junctions (TJs) in mammals and septate junctions (SJs) in insects. Specialized TJs/SJs, called tricellular junctions (TCJs), are located at the nexus of three adjacent cells, and we have shown that aging results in changes to TCJs in intestines of adult *Drosophila melanogaster*. We now demonstrate that localization of the TCJ protein bark beetle (Bark) decreases in aged flies. Depletion of *bark* from enterocytes in young flies led to hallmarks of intestinal aging and shortened lifespan, whereas depletion of *bark* in progenitor cells reduced Notch activity, biasing differentiation toward the secretory lineage. Our data implicate Bark in EC maturation and maintenance of intestinal barrier integrity. Understanding the assembly and maintenance of TCJs to ensure barrier integrity may lead to strategies to improve tissue integrity when function is compromised.

INTRODUCTION

The intestinal barrier allows selective paracellular transport of water, ions, and nutrients while maintaining food and microbes inside the intestinal lumen.[1] Barrier integrity is crucial to intestinal homeostasis because leakage of potentially harmful antigens or microbes could be detrimental to interstitial tissues. There is a strong correlation between aging and decline in intestinal barrier integrity across multiple species, including *Drosophila melanogaster*.[2–7] Age-associated loss of the intestinal barrier in *Drosophila* is associated with systemic metabolic defects, such as changes in insulin/insulin-like growth factor signaling, intestinal dysbiosis, chronic expression of inflammatory genes, and an increase in proliferation of intestinal stem cells (ISCs).[7–9] Intercellular occluding junctions, referred to as tight junctions (TJs) in vertebrates and septate junctions (SJs) in arthropods, play a major role in maintenance of the intestinal barrier.[10–12] Although TJs and SJs appear different ultrastructurally, they share many homologous proteins, and both TJs and SJs restrict passive, paracellular transport. TJs use a branched network of independently sealing strands to create a semipermeable barrier at "kissing points" between adjacent membranes, whereas SJs reduce net solute diffusion by increasing diffusional distance across the junction with bridge-like structures called septa.[13,14] In *Drosophila*, pleated SJs (pSJs) are found in epithelia derived from ectoderm, whereas smooth SJs (sSJs) are found in endoderm-derived tissues, such as the midgut.[15–17] Similar to TJs, sSJs in *Drosophila* are located apical to adherens junctions,[17] making the *Drosophila* midgut a tractable model system for studying mammalian TJs, such as those that maintain the mammalian intestinal barrier.

The *Drosophila* posterior midgut (PMG) is functionally analogous to the human small intestine.[18] The PMG epithelium is composed primarily of absorptive enterocytes (ECs), polyploid cells with microvilli that extend into the gut lumen and facilitate the absorption of nutrients. ECs and secretory enteroendocrine (EE) cells are maintained by a pool of ISCs that are able to self-renew by producing new ISCs. ISCs primarily generate daughter enteroblasts (EBs), which then differentiate into either mature ECs or EE cells.[18] EB fate is specified by activation of the Notch signaling pathway,[19,20] leading to the expression of the transcription factor *klumpfuss (klu)* in EBs. EE cell and EC fate decisions become stochastic on loss of lineage specifying *klu*, and EB fates can be tracked using specific *klu*-based lineage tracing tools (e.g. *klu*^*ReDDM*^).[21,22]

[1]Department of Molecular, Cell and Developmental Biology, University of California, Los Angeles, Los Angeles, CA 90095, USA

[2]Institute of Genetics, Heinrich-Heine-University, Düsseldorf, Germany

[3]Eli and Edythe Broad Center of Regenerative Medicine and Stem Cell Research, University of California, Los Angeles, Los Angeles, CA 90095, USA

[4]Department of Anatomy, University of California, San Francisco, CA 94143, USA

[5]Department of Medicine, Division of Geriatrics, University of California, San Francisco, CA 94143, USA

[6]Bakar Aging Research Institute, University of California, San Francisco, San Francisco, CA 94143, USA

[7]Lead contact

*Correspondence: leanne.jones@ucsf.edu

https://doi.org/10.1016/j.isci.2023.106901

In aged flies, ISC proliferation increases dramatically, as measured by an increase in cells that are positive for the mitotic marker phospho-histone H3 (pHH3).[3,23–26] The increase in progenitor cells is coupled with a delay in differentiation, resulting in an accumulation of cells co-expressing the ISC/EB markers Escargot, Delta, and reporters of the Notch signaling pathway.[3] Smooth SJs are found between adjacent ECs and between ECs and EE cells, and our lab has demonstrated previously that integrity of sSJs between ECs is required for maintenance of the intestinal barrier in the midgut.[10] Thus, additional intestinal phenotypes exhibited by aged flies include loss of sSJ physical integrity (visible gaps between membranes)[10] and loss of the intestinal barrier.[7] Indeed, electron micrographs of ECs in aged flies revealed gaps between adjacent ECs, suggesting a loss of sSJ integrity over time.[10] Gaps in SJs correlated with changes in localization of key sSJ components in PMGs from old flies. Immunofluorescence (IF) imaging revealed decreased staining intensity for several sSJ components at the junction, relative to the cytoplasm, with a concomitant increase in staining intensity in the cytoplasm, relative to what was observed for cells in intestines from young flies.[10]

In *Drosophila*, specialized junctions, referred to as tricellular junctions, are found where three adjacent cells meet. Similar to sSJ proteins, the tricellular septate junction (tSJ) protein Gliotactin (Gli) was lost from the tSJ and increasingly localized to cytoplasmic puncta in ECs from aged flies.[10] Bark beetle (Bark), another tSJ-specific protein, also referred to as Anakonda, is required for proper Gli localization to the tSJ in the fly embryonic epithelium. Bark and Gli colocalize at the tSJ in both pSJs and sSJs.[27,28] Because Gli is required at tSJs between ECs to maintain intestinal homeostasis,[10] and because proper Gli localization was disrupted in aged flies, we wanted to determine whether Bark also plays a role in the adult intestine. Here, we show that Bark localizes to the tSJ and that it is required in both EBs and mature ECs to maintain intestinal homeostasis.

RESULTS

Bark is expressed in the adult intestine

Bark is a type I transmembrane protein with a tripartite extracellular domain; it has been proposed that Bark forms a trimer, which acts as a diaphragm in the center of the tSJ canal.[27] Bark was demonstrated to be required for proper localization of Gli and maturation of the pSJ in the embryonic epithelium.[27] To determine whether Bark has a role in the adult intestine, PMGs from young (2 do) flies expressing a GFP-tagged form of Bark (hereafter referred to as Bark::GFP, see STAR Methods)[29] were stained with anti-Bark antibody.[28] Bark localized to tSJs in both the PMG and hindgut, similar to what was observed in the embryonic epithelium[27] (Figures 1, S1, and 2A). Specifically, in the PMG, Bark localized to the tSJ between adjacent ECs and ECs and EE cells. By contrast, in aged (40-day-old, do) flies, Bark localization decreased at the tSJ between adjacent ECs and appeared to spread along the bicellular junction, with modest accumulation in the cytoplasm (Figures 2B, 2B', and 2C). Loss of Bark from the tSJ in PMGs from aged flies is similar to what was observed for Gli; however, previous studies indicated significantly more accumulation of Gli in the cytoplasm, when compared to Bark.[10]

Given the previously described relationship between Bark and Gli, where Bark is required for recruitment of Gli to the tSJ in developing embryonic epithelia,[27] we wanted to determine whether Bark is required for Gli localization in the adult PMG. As mutations in *bark* are embryonic lethal, we took advantage of an inducible gene expression system, GeneSwitch (GS), to deplete *bark* from ECs, specifically in young adult flies. The GeneSwitch (GS) system permits cell type-specific gene expression following feeding flies the progesterone analog mifepristone (RU-486).[30,31] Similar to previously published results in the embryonic epithelium,[27] RNAi-mediated depletion of *bark* in ECs in midguts of young flies resulted in a decrease in Gli::GFP staining intensity at the tSJ (Figures 3A and 3B''). However, in contrast to the findings in the embryonic epithelium, depletion of *Gli* resulted in an increase in Bark::GFP staining intensity at the bicellular junction, somewhat reminiscent of the localization observed in guts from aged flies (Figures 2B–2B' and 3C–3D''). A similar, mutually dependent relationship between Gli and Bark has been observed in the pupal notum.[32] In addition, depletion of either *bark* or *Gli* non-autonomously increased ISC proliferation (Figures 3E, 3F and 4A–4C) and Gli depletion reduced Bark::GFP staining at TCJ (Figure 3G), as observed in old flies (Figure 2C). Taken together, these data suggest that the mechanisms for assembly and maintenance of the tSJ may differ by tissue type and/or with age.

bark is required in ECs for the maintenance of intestinal homeostasis

Given that the changes in Gli::GFP on depletion of *bark*, and vice versa, resemble what occurs at the tSJ in an aged midgut, we wanted to determine whether depletion from ECs in PMGs from young flies led to other aging phenotypes. Following depletion of *bark* from ECs in young flies for 5 days, the number of pHH3+ cells was
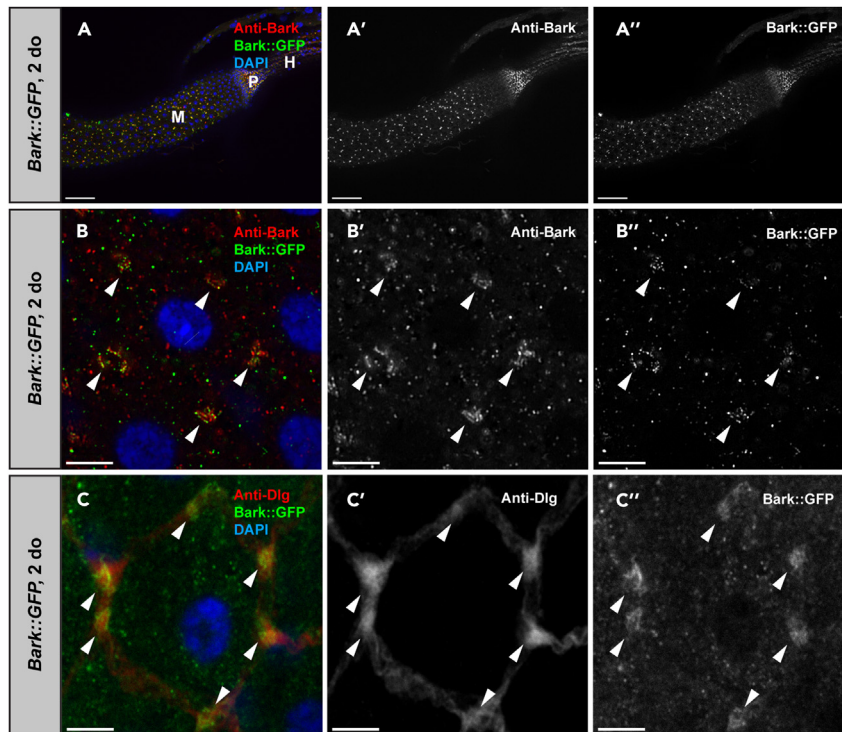
Figure 1. Anakonda/Bark beetle (Bark) localizes to the tricellular septate junction (tSJ) in the adult *Drosophila* intestine

(A–A″) Representative staining for Bark (antisera, red) (*Bark::GFP*, GFP, green) in the posterior midgut (M) of young (2 do) flies. Pylorus (P) and hindgut (H) to the right. DNA is stained with DAPI (blue). Scale bars, 50 μm.

(B–B″) High magnification view of an enterocyte (EC) showing staining of endogenous Bark protein and GFP-tagged Bark at the tSJ (arrowheads). Scale bars, 5 μm.

(C–C″) High magnification view of an EC showing GFP-tagged Bark colocalizes with the bicellular septate junction (bSJ) protein Discs large 1 (Dlg1, red) at the tSJ (arrowheads). Scale bars, 5 μm.

significantly higher than in controls (Figures 3E, 3F and 4 A–4C), suggesting that Bark is required in ECs to maintain intestinal homeostasis, similar to Gli (Figure 3F).[10] Immunostaining confirmed depletion of Bark protein from ECs using the *5966^GS* driver, validating the RNAi line (Figures S2A and S2B). In addition, the number of pHH3$^+$ cells increased with extended induction times (Figures S2E–S2G). Similar results were obtained using additional, independent *RNAi* lines (Figures 4C, S2C–S2D′, S2H–S2K), as well as alternative, inducible systems to deplete *bark* from ECs (i.e., *Myo1A-GAL4^ts*, Figures S2H–S2K). As a result of increased ISC proliferation, depletion of *bark* in ECs also increased total cell number (Figure S2J) and progenitor cell numbers, as indicated by *esg$^+$* cells (Figure S2K), suggesting disrupted intestinal homeostasis.

Next, we wanted to determine whether Bark is required for maintenance of the intestinal barrier, similar to Gli.[10] The GeneSwitch system was used to deplete *bark* in ECs throughout the adult lifespan. Integrity of the intestinal barrier and lifespan were assayed in parallel by feeding the flies a non-absorbable, non-toxic blue food dye as described previously.[7,33] In flies with an intact intestinal barrier, the dye remains in the lumen of the digestive tract; however, when the intestinal barrier is severely compromised, the dye visibly leaks into the hemolymph.[33] Consistent with a model in which Bark plays an integral role in tSJs, depletion of *bark* in ECs led to significant loss of the intestinal barrier after 19 days. Furthermore, as has been demonstrated previously, loss of barrier integrity correlated with shortened lifespan, when compared to control flies (Figures 4D and 4E).[7] These data indicate that Bark is required in ECs for regulating intestinal homeostasis, maintaining the intestinal barrier, and for a normal lifespan.

bark is required in EBs for proper differentiation

One hallmark of the aging PMG is accumulation of EB-like cells that express hallmarks of both ISCs and ECs.[3,24] Although Bark expression was detected at tSJs between ECs and EEs, single cell sequencing
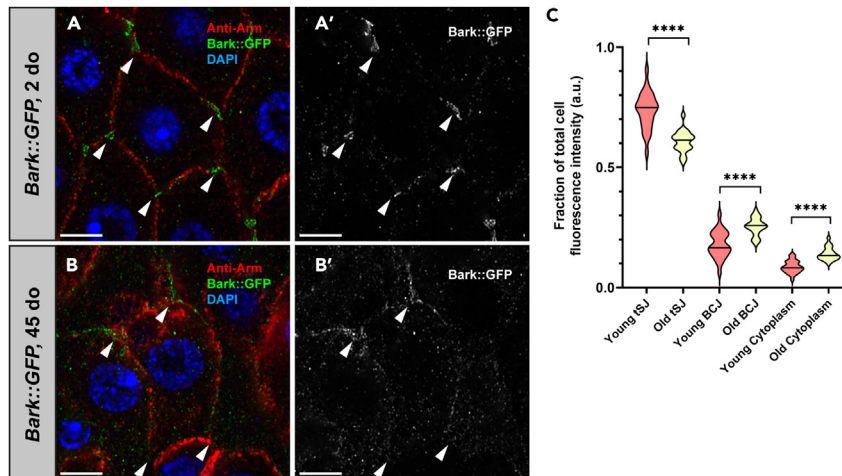
Figure 2. Bark is lost from the tSJ in aged flies

(A) In young (2 do) flies, Bark localizes to the tSJ (arrowheads) in ECs, whereas it is no longer detected at the tSJ in the aged (45 do) flies. Scale bars, 5 µm.

(B and B') Adherens junctions (Armadillo, Arm, red); Bark (GFP, green); DNA (DAPI, blue). Scale bars, 5 µm.

(C) Quantification reveals that Bark is increased at the bicellular septate junction (bSJ) or in the cytoplasm of old flies. 3 cells were analyzed per PMG. young, n = 26; old, n = 22. 3 cells were measured per PMG. Each clearly visible tSJ in the cell was measured. 6 measurements were taken of the BCJ and cytoplasm in each cell, respectively. Quantification of fluorescence intensity ratios for Bark (C) in the bicellular junction (BCJ), tSJ, and cytoplasm. Black lines indicate median; statistical significance determined by Mann-Whitney test. ns, not significant; *, $p < 0.05$; **, $p < 0.001$; ****, $p < 0.0001$.

data revealed expression of *bark* in EBs.[34,35] Therefore, we wanted to investigate a role for *bark* in progenitor cells committed to the EC lineage by combining conditional expression of *bark* RNAi with an established lineage tracing approach, ReDDM.[21,22] Briefly, *klu*[ReDDM] utilizes different fluorophore stabilities in combination with EB-specific manipulation and tracing of differentiated ECs (see STAR Methods for more information).[21,22] Depleting *bark* using *klu*[ReDDM] resulted in accumulation of *klu*[+] EBs (Figures 5A, 5B''' and 5E), although not at the expense of EC differentiation (Figures 5F and 5G). Similar results were obtained when *bark* was depleted from ISCs and EBs using another ISC/EB driver (*esg*[ReDDM]) (Figure S3).[36] Furthermore, specific depletion of *bark* from EBs reduced lifespan compared to outcrossed controls (Figures 5J and 5K) and increased loss of epithelial barrier integrity, similar to depletion in ECs. Importantly, reduction in lifespan was not caused by persistent depletion of *bark* in ECs, as traced, newly differentiated ECs show Bark::GFP localized at the TCJ (Figures S4A–S4B''). Depletion of *bark* in EBs also led to an increase in newly generated EEs, identified by antibody staining for the EE marker Prospero (Pros[+], Figure 5H), and a non-autonomous increase in ISC proliferation (pHH3[+], Figures 5C, 5D' and 5I). Similar to our observations of ECs in intestines from aged flies,[10] EB-specific depletion of *bark* reduced immunofluorescence staining intensity of the SJ marker Dlg1 at the bSJ (Figures S4C–S4E).

Cell fate decisions after ISC division strongly depend on the Notch signaling pathway, whereby low Notch activation was shown to drive EE differentiation.[19,20,37] By using *Su(H)-GBE-GFP* as a reporter of Notch activation,[38] we found that depletion of *bark* using *klu-GAL4* led to a reduction in *Su(H)-GBE-GFP* fluorescence intensity (Figures 6A–6C) and smaller EB nuclei (Figure 6D). Indeed, intestines of aged flies (45 do) contain more EBs (Figures 6E, 6F and 6H) with reduced Notch-activity (Figure 6G), phenocopying *bark* depletion from EBs. Therefore, our data indicate that on *bark* depletion, EBs demonstrate an increased propensity to differentiate along the EE lineage, which has previously been observed on loss of the lineage marker *klu* in EBs.[21,22] Taken together, our findings suggest that Bark plays a role during EB to EC differentiation and that depletion of *bark* leads to accumulation of EBs with reduced Notch activity, increasing differentiation toward EE fate.

DISCUSSION

Occluding junctions, known as tight junctions in mammals and septate junctions in arthropods, play a significant role in maintaining the intestinal barrier,[1,10,11] which passively restricts paracellular flow across the
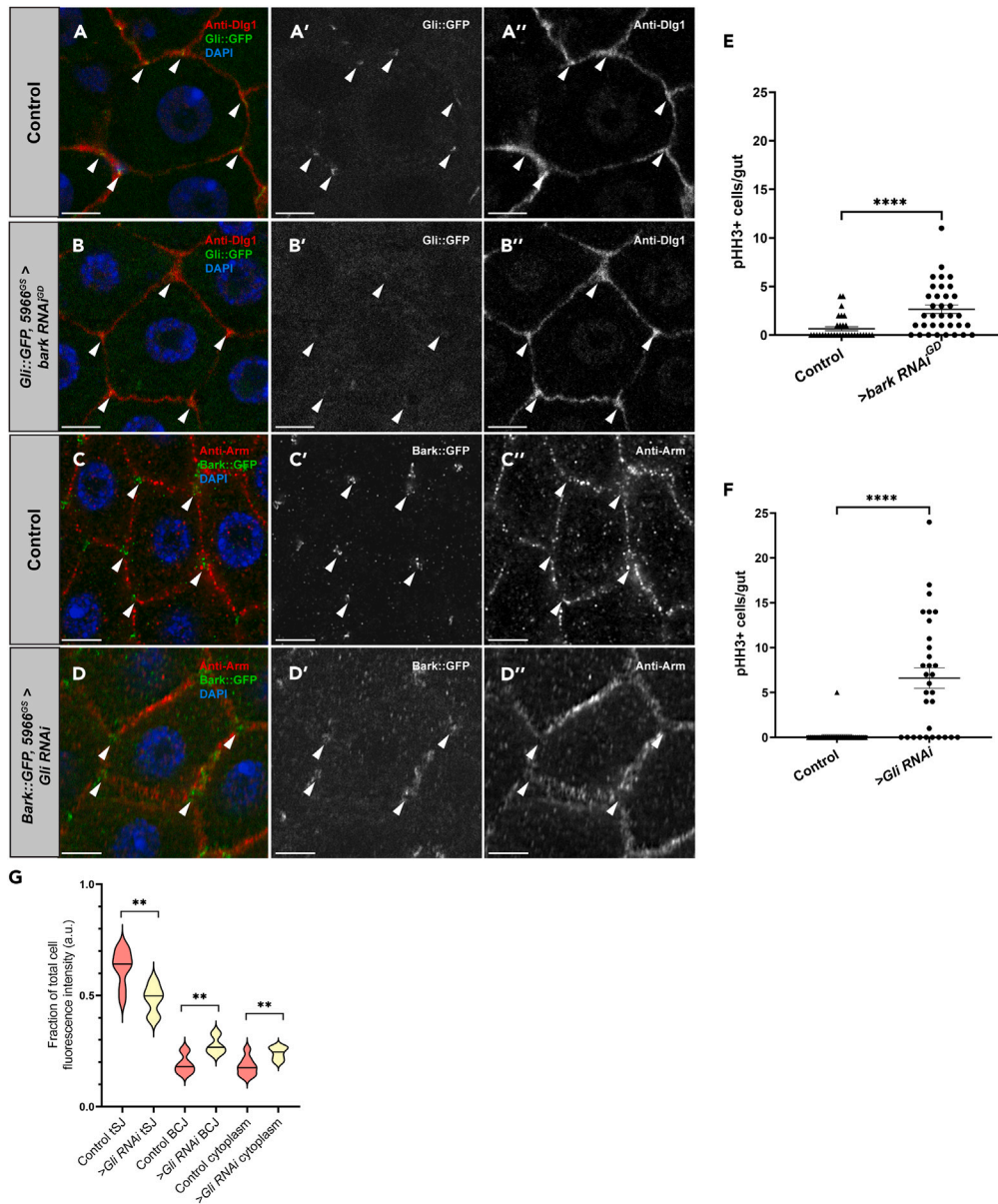
Figure 3. Depletion of Gli results in loss of Bark from the tSJ in the adult posterior midgut

(A–A″) In young outcrossed fly PMGs, Gli localizes exclusively to the tSJ. Scale bars, 20 μm.

(B–B″) EC-specific depletion of Bark protein by 5966^{GS};bark $RNAi^{GD}$ expression causes mislocalization of Gli to cytoplasmic puncta, indicating Bark is required for Gli localization to the tSJ in the PMG. Genotypes: *w; Gli::GFP; bark RNAi^{GD}* (control); *w; Gli::GFP; 5966^{GS};bark RNAi^{GD}*. All flies are fed RU-486 for 7 days to induce transgene expression. Scale bars, 20 μm.

(C–C″) In young outcrossed (7 do) fly PMGs, Bark is localized exclusively to the tSJ. Scale bars, 20 μm.

(D–D″) Depletion of Gli expression in ECs of young (7 do) flies leads to loss of Bark from the tSJ and an increase in Bark on the bicellular junction and cytoplasm. Genotypes: *w; 5966^{GS}* (control); *w; Bark::GFP, 5966^{GS};Gli RNAi*. All flies are fed RU-486 for 5 days to induce transgene expression. Bark (GFP, green); Armadillo (Arm, adherens junctions, red); DNA (DAPI, blue). Scale bars, 20 μm.

(E) Quantification of mitotic events in the posterior midguts of 5966^{GS};bark $RNAi^{GD}$ and outcrossed controls. Median ±SEM; statistical significance was determined by Mann-Whitney test. ****, $p < 0.0001$.

(F) Quantification of mitotic events in the posterior midguts of 5966^{GS};Gli RNAi and outcrossed controls. Median ±SEM; statistical significance was determined by Mann-Whitney test. ****, $p < 0.0001$.

(G) Quantification of fluorescence intensity ratios for Bark in the bicellular junction (BCJ), tSJ, and cytoplasm. Black lines indicate median; Statistical significance determined by Mann-Whitney test. **, $p < 0.01$.
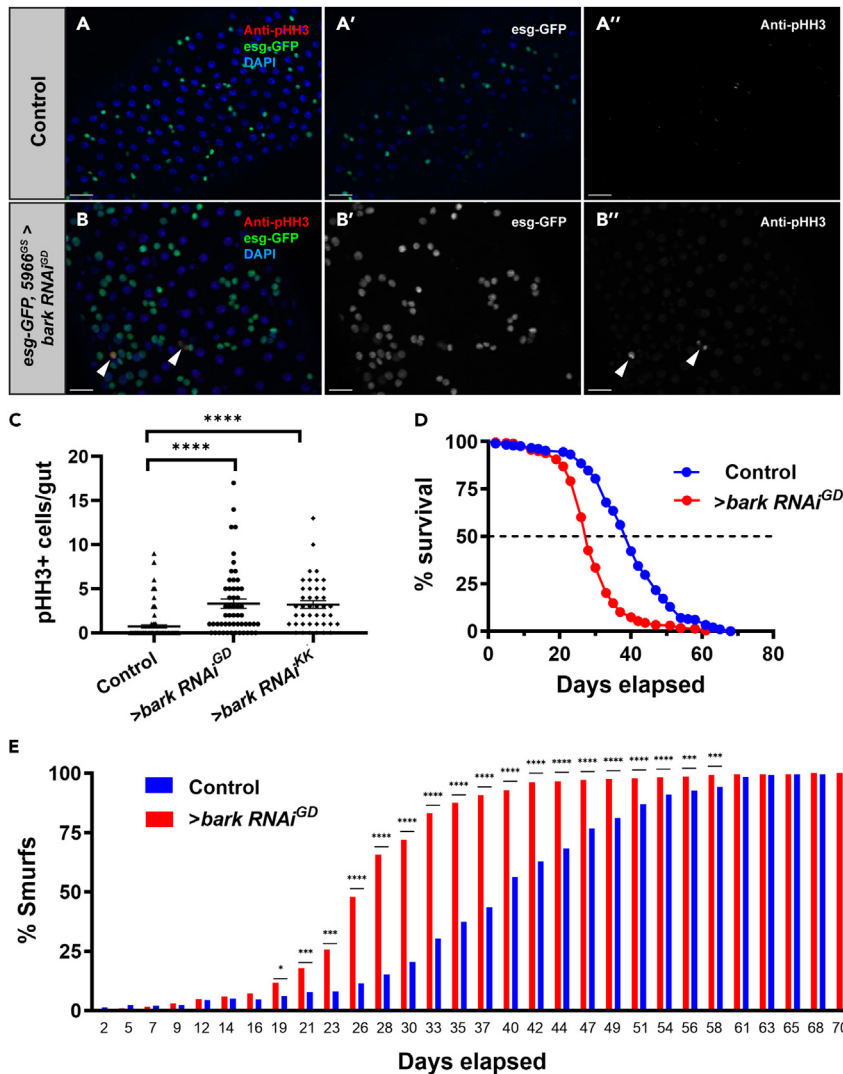
Figure 4. Bark is required at the tSJ in enterocytes to maintain intestinal homeostasis

(A and B) Depletion of Bark in ECs of young (2 do) flies by 5966^{GS};*bark RNAi^{GD}* expression for 5 days results in an increase in mitotic activity (n = 54), compared to outcrossed controls (n = 48). Genotypes: (A) *w; esg-GFP, 5966^{GS}* (B) *w; esg-GFP, 5966^{GS};bark RNAi^{GD}*. All flies are fed RU-486 to induce transgene expression. ISCs/EBs (GFP, green); mitotic cells (phosphorylated histone H3, pHH3, red), DNA (DAPI, blue). Scale bars, 20 μm.

(C) Quantification of mitotic events. *w; esg-GFP, 5966^{GS};bark RNAi^{KK}* flies are also included (n = 42). Error bars represent mean with SEM. Median ±SEM; statistical significance was determined by Mann-Whitney test. ****, $p < 0.0001$.

(D and E) Intestinal barrier integrity assay shows loss of barrier function upon depletion of Bark (red, n = 301) and (D) statistically significant (****) shortening of lifespan, when compared to outcrossed controls (blue, n = 299). Genotypes: Red, *w; esg-GFP, 5966^{GS}>UAS-bark RNAi^{GD}*; blue, *w; esg-GFP, 5966^{GS}*. *, $p < 0.05$; ***, $p < 0.001$, ****, $p < 0.0001$. Statistical significance determined by Fisher's exact test (barrier integrity assay) and non-parametric log rank Mantel-Cox test (lifespan assay).

intestinal epithelium. Of interest, loss of the intestinal barrier has been described as a result of aging and is associated with impending death across species.[7] Owing to the strong correlation between aging and loss of the intestinal barrier,[2–7] we wanted to characterize the impact of aging on occluding junctions, using the *Drosophila* intestine as a model system. Here, we describe the expression, localization and role of the tSJ component Bark in the adult PMG.

Bark localized to the tSJ in both the PMG and hindgut (Figures 1, and S1); however, analysis of PMGs from aged flies indicated that Bark was lost from the tSJ over time (Figure 2). Concomitant with the decreased
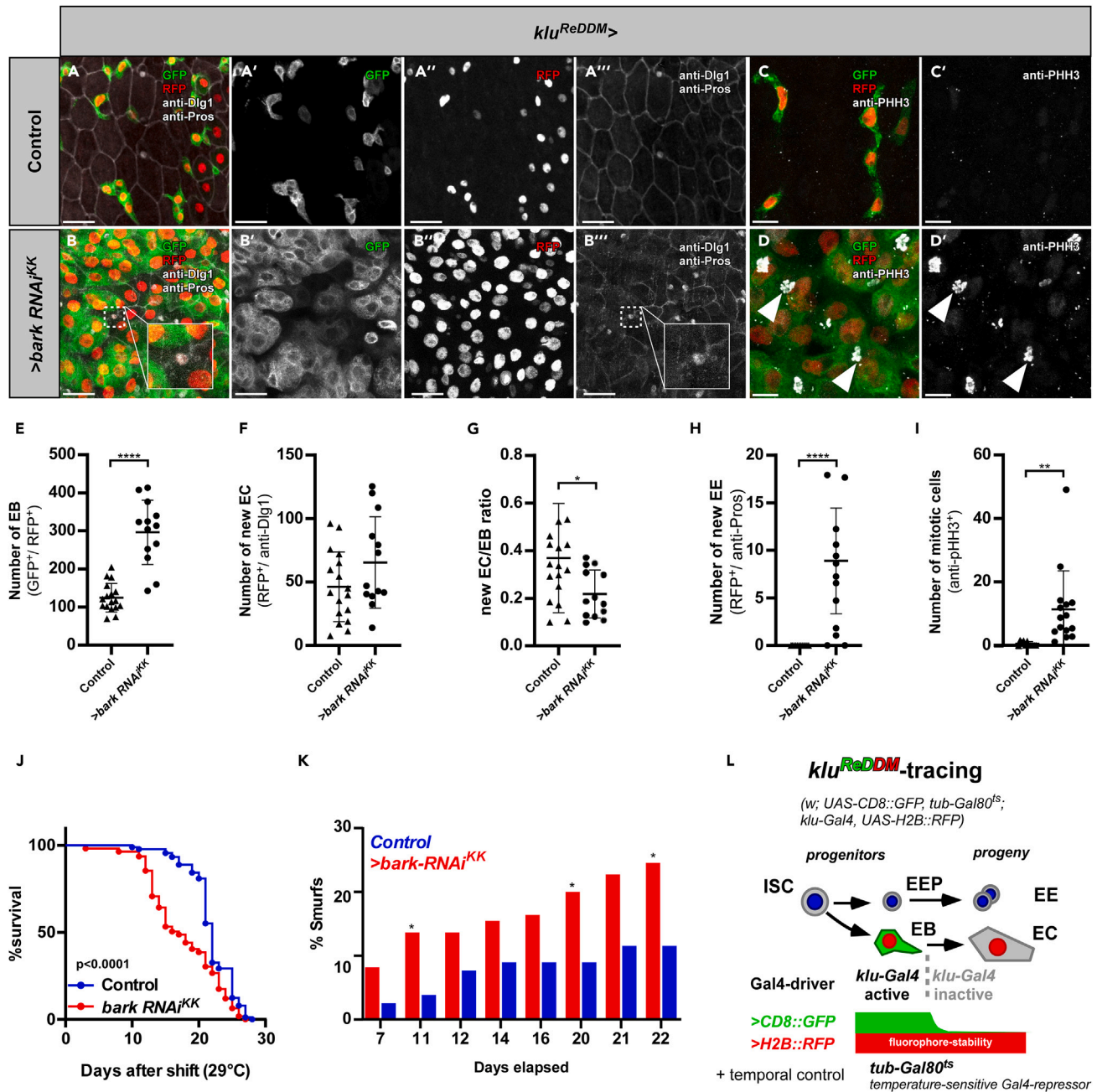
Figure 5. EB-specific depletion of *bark* results in EB accumulation, EE fate plasticity, and increases epithelial permeability

(A–B‴) Confocal images of control PMGs (A-A‴) and >*bark RNAi^KK* (B-B‴) in the R5 region after 7 days of tracing. Scale bar 20 μm.

(C–D′) Knockdown of *bark* (D-D′) leads to an increase in the number of proliferating cells (marked by pHH3) as compared to the controls (C-C′). Scale bar 10 μm.

(E–H) Quantifications of the number of EBs (E), new ECs (F), and traced EEs (H) on *bark* knockdown after 7 days of tracing. Depletion of *bark* induces EB to EE differentiation (insert, GFP⁻/RFP⁺/anti-Pros⁺, H) but no significant change in the number of ECs (GFP⁻/RFP⁺/anti-Dlg1⁺, F). (Control n = 17, >*bark RNAi^KK* n = 13). Mean ± SD; statistical significance was determined by Mann-Whitney test. ****, p < 0.001. In addition, *bark* knockdown increased the number of progenitor cells (GFP⁺/RFP⁺, E). Mean ± SD; statistical significance was determined by Mann-Whitney test. ****, p < 0.001. (G) EC/EB ratio decreases upon *bark* knockdown. (Control n = 17, >*bark RNAi^KK* n = 13). Mean ± SD; statistical significance was determined by Mann-Whitney test. *, p < 0.05.

(I) Quantification of the number of mitotic cells on *bark* depletion after 7 days of tracing. (control n = 11, >*bark RNAi^KK* n = 15). Mean ± SD; statistical significance was determined by Mann-Whitney test. **, p < 0.01.

Figure 5. *Continued*

(J) Survival (in percentage) over time on bark knockdown using *klu^ReDDM*. Survival curves were plotted by combining data from >80 flies per one genotype group: Control (blue, n = 89), *bark RNAi^KK* (red, n = 109). *bark* knockdown in EBs reduces lifespan significantly. Statistical significance determined by non-parametric log rank Mantel-Cox test. ****, p < 0.0001.

(K) Intestinal barrier integrity assay shows loss of barrier function upon depletion of Bark (red, n = 110) when compared to outcrossed controls (blue, n = 81). Statistical significance determined by Fisher's exact test.

(L) *klu^ReDDM* (*w; UAS-CD8::GFP, tub-GAL80^ts; klu-GAL4; UAS-H2B::RFP*) tracing. Expression of two fluorophores (*CD8::GFP* and *H2B::RFP*) is driven by EB-specific driver *klu-GAL4*. EBs differentiating to epithelial ECs lose *CD8::GFP*, while stable *H2B::RFP* persists. The expression of UAS-driven transgenes is temporally controlled by a ubiquitously expressed temperature-sensitive *GAL80^ts* repressor, which is inactivated by temperature shift to 29°C.

staining intensity at the tSJ, we observed an increase in staining along the bicellular junction (Figure 2). Depletion of *bark* from ECs in young flies led to an increase in ISC proliferation, loss of the intestinal barrier, and shortened lifespan (Figures 3 and 4). These results are similar to what we reported previously for another tSJ component, Gli.[10] Although our study utilizes RNAi-mediated depletion of tSJ components, we have shown previously that transcription of *bark* does not decrease with age in the PMG[10]; therefore, our approach may not accurately recapitulate the impact of aging on the tSJ. However, these studies are a relevant first step toward understanding the importance of Bark and other SJ proteins in intestinal homeostasis.

Our finding that Bark is lost from the tSJ in PMGs from aged flies, in combination with the observation that depletion of *bark* from ECs in young flies recapitulates some prevalent intestinal phenotypes that are apparent with age, supports the hypothesis that loss of SJ components may contribute to age-related loss of intestinal barrier function.[10,11] One possible mechanism leading to age-related changes in the localization of SJ proteins could be alterations in vesicular trafficking, including increased endocytosis of SJ proteins and/or decreased delivery of recycled or newly synthesized SJ proteins to the plasma membrane. Manipulation of transport machinery, rather than production of SJ proteins, could be explored as an approach to restore Bark and other SJ proteins at the SJ in aged flies; however, manipulation of transport machinery would likely result in pleiotropic, unrelated phenotypes.

In addition to analyzing a role for Bark in ECs, we show that EB-specific depletion of *bark* results in accumulation of EB-like cells, resembling defects observed in flies that are aged or have damaged intestinal epithelia.[39,40] The accumulation of EB-like cells correlated with a decrease in lifespan (Figures 5B and 5E), as reported previously.[36] EBs depleted for *bark* are capable of forming ECs in normal numbers (Figure 5F), although cells originating from Bark-depleted EBs are abnormally small (Figures 6A–6B and 6D), show irregular Dlg1 localization (Figures S4C–S4E) and fate is shifted toward the EE lineage (Figure 5H). Therefore, we speculate that depletion of *bark* from EBs results in failure to form proper contact with existing ECs, which delays EB differentiation, leading to their accumulation. Interestingly, Bark expression following transient knockdown of *bark* in EBs is rescued in new (i.e., linage-traced) ECs, as they show normal Bark::GFP at tSJ. Our findings indicate an essential role for Bark during tSJ establishment when differentiating EBs integrate into the intestinal epithelium. Future studies will focus on an ultrastructural study of Bark localization in late EBs, achieving a better understanding of how Bark may participate in recently identified apical membrane initiation sites[41] whereas EBs undergo epithelial integration, acting to establish and preserve intestinal barrier function.

In our evaluation of the relationship between Gli and Bark protein in the PMG tSJ, we found that depletion of one component results in changes in staining intensity of the other at tSJs in adult PMGs (Figure 3). Our findings are different from previous studies that examined the relationship between Bark and Gli in the embryonic epithelium,[27] which found Bark is required for Gli to localize to the TCJ, whereas the reverse was not true. However, another study revealed Gli and Bark are mutually dependent for localization to the tSJ in the pupal notum.[32] Differences could be because of relationships between Gli and Bark in embryonic versus adult tissues, the use of null alleles versus RNAi-mediated depletion, time of RNAi depletion, and/or the use of antibodies targeting the proteins directly, rather than GFP tags. An ultrastructural study could better pinpoint the nature of Gli-Bark interaction in the PMG. Investigation of the relationship between Gli and Bark to another tSJ protein, M6[32,42] in the *Drosophila* PMG may also help further illuminate these differing results.

In summary, we have found that Bark protein is required in the tSJs of ECs and EBs in the *Drosophila* posterior midgut to maintain homeostasis with respect to ISC proliferation, EB fate, intestinal barrier function, and lifespan. Because Bark also mislocalizes from the tSJ in the aged fly PMG, our study suggests that this mislocalization may contribute to the overall intestinal aging phenotype. In addition, Bark and the tSJ
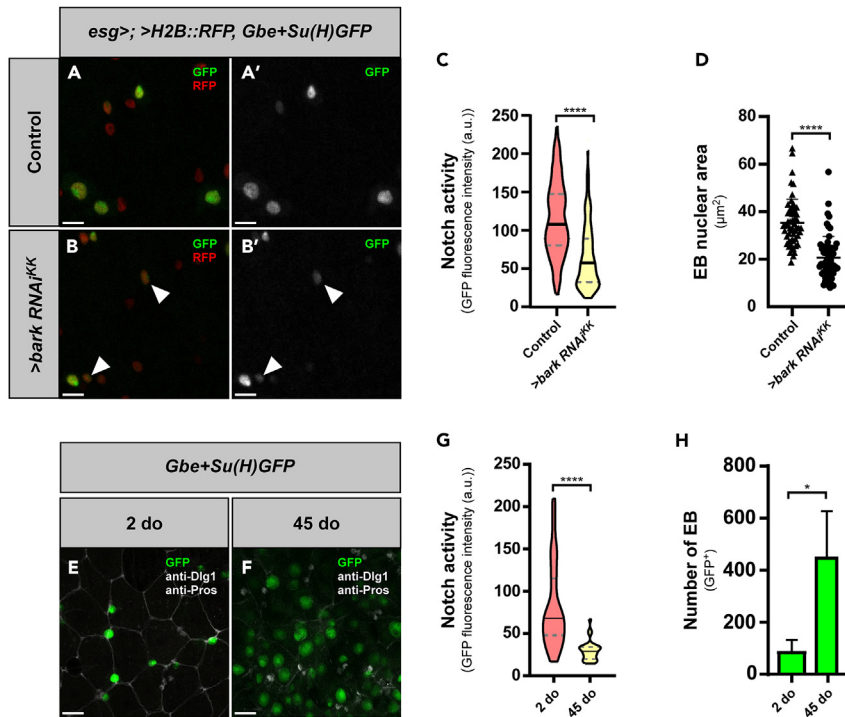
Figure 6. Knockdown of *bark* in ISCs/EBs results in reduced Notch pathway activation, similar to aging

(A–B') Expression of *H2B::RFP* is driven by ISC- and EB- driver *esg-GAL4*. H2B::RFP persists in epithelial ECs differentiated from EBs. *Gbe+Su(H)GFP* is a readout of Notch activity and a marker of the EB lineage (arrowheads, B-B') Scale bar, 10 um.

(C and D) Quantification of GFP fluorescence intensity and (D) EB nuclear size following 7 days of *bark* depletion. Knockdown of *bark* decreases GFP fluorescence intensity (C) and EB nuclear size (GFP+ cells, D) compared to controls (control n = 73, *>bark RNAi*KK n = 70). Mean ± SD; statistical significance determined by Mann-Whitney test. ****, $p < 0.0001$.

(E and F) In aged (45 do) flies (F), EB number (GFP+ cells) is higher than in young (2 do) flies (E). (arrowheads, B-B')
Scale bar, 10 um.

(G and H) Quantification of GFP fluorescence intensity and (H) EB number following 7 days of *bark* depletion. Knockdown of *bark* decreases GFP fluorescence intensity (control n = 27, *>bark RNAi*KK n = 30) (G) and increases EB number (GFP+ cells, control n = 3, *>bark RNAi*KK n = 3) compared to controls (H). Mean ± SD; statistical significance determined by Student's *t* test. *, $p < 0.05$, ****, $p < 0.0001$.

protein Gliotactin appear mutually dependent on one another for proper tSJ localization in the adult PMG, unlike in the embryonic epithelium.[27] Given the importance of intestinal barrier function, and age-related intestinal barrier loss across species,[2–7] our discovery of an essential role for Bark during homeostatic cellular turnover sheds light on fascinating future research lines. This study could help generate insight into the role of tSJs in the human gut and possible pathologies associated with tSJ dysfunction.

Limitations of the study

Because RNAi-based knockdowns may not be fully penetrant, a potential caveat is that depletion of Bark may not fully recapitulate aging phenotypes. In addition, because Bark protein is not readily detected in EBs, it is difficult to determine exactly what the role of Bark may be in EBs. However, we speculate that expression of Bark at the EB-EC transition is critical for the initial assembly of tricellular junctions in the adult intestine.

STAR★METHODS

Detailed methods are provided in the online version of this paper and include the following:

- KEY RESOURCES TABLE
- RESOURCE AVAILABILITY
  - Lead contact
  - Materials availability
  - Data and code availability

SUPPLEMENTAL INFORMATION

Supplemental information can be found online at https://doi.org/10.1016/j.isci.2023.106901.

AUTHOR CONTRIBUTIONS

R.A.H., M.G., and M.R-D. designed, performed, and analyzed experiments and edited the manuscript. E.E., F.de la T., C.D., and N.H.K. performed experiments. T.R and D.L.J. designed and analyzed experiments and wrote the manuscript.

DECLARATION OF INTERESTS

The authors declare no competing interests.

INCLUSION AND DIVERSITY

One or more of the authors of this paper self-identifies as an underrepresented ethnic minority in their field of research or within their geographical location. One or more of the authors of this paper received support from a program designed to increase minority representation in their field of research.

REFERENCES

1. Marchiando, A.M., Graham, W.V., and Turner, J.R. (2010). Epithelial barriers in homeostasis and disease. Annu. Rev. Pathol. *5*, 119–144.

2. Kirkwood, T.B.L. (2004). Intrinsic ageing of gut epithelial stem cells. Mech. Ageing Dev. *125*, 911–915.

3. Biteau, B., Hochmuth, C.E., and Jasper, H. (2008). JNK activity in somatic stem cells causes loss of tissue homeostasis in the aging *Drosophila* gut. Cell Stem Cell *3*, 442–455.

4. Ren, W.y., Wu, K.f., Li, X., Luo, M., Liu, H.c., Zhang, S.c., and Hu, Y. (2014). Age-related changes in small intestinal mucosa epithelium architecture and epithelial tight junction in rat models. Aging Clin. Exp. Res. *26*, 183–191.

5. Schiffrin, E.J., Morley, J.E., Donnet-Hughes, A., and Guigoz, Y. (2010). The inflammatory status of the elderly: the intestinal contribution. Mutat. Res. *690*, 50–56.

6. Tran, L., and Greenwood-Van Meerveld, B. (2013). Age-associated remodeling of the intestinal epithelial barrier. J. Gerontol. A Biol. Sci. Med. Sci. 68, 1045–1056.

7. Rera, M., Clark, R.I., and Walker, D.W. (2012). Intestinal barrier dysfunction links metabolic and inflammatory markers of aging to death in Drosophila. Proc. Natl. Acad. Sci. USA 109, 21528–21533.

8. Clark, R.I., Salazar, A., Yamada, R., Fitz-Gibbon, S., Morselli, M., Alcaraz, J., Rana, A., Rera, M., Pellegrini, M., Ja, W.W., et al. (2015). Distinct shifts in microbiota composition during Drosophila aging impair intestinal function and drive mortality. Cell Rep. 12, 1656–1667.

9. Guo, L., Karpac, J., Tran, S.L., and Jasper, H. (2014). PGRP-SC2 promotes gut immune homeostasis to limit commensal dysbiosis and extend lifespan. Cell 156, 109–122.

10. Resnik-Docampo, M., Koehler, C.L., Clark, R.I., Schinaman, J.M., Sauer, V., Wong, D.M., Lewis, S., D'Alterio, C., Walker, D.W., and Jones, D.L. (2017). Tricellular junctions regulate intestinal stem cell behaviour to maintain homeostasis. Nat. Cell Biol. 19, 52–59.

11. Salazar, A.M., Resnik-Docampo, M., Ulgherait, M., Clark, R.I., Shirasu-Hiza, M., Jones, D.L., and Walker, D.W. (2018). Intestinal snakeskin limits microbial dysbiosis during aging and promotes longevity. iScience 9, 229–243.

12. Izumi, Y., Furuse, K., and Furuse, M. (2019). Septate junctions regulate gut homeostasis through regulation of stem cell proliferation and enterocyte behavior in Drosophila. J. Cell Sci. 132, 232108.

13. Mariano, C., Sasaki, H., Brites, D., and Brito, M.A. (2011). A look at tricellulin and its role in tight junction formation and maintenance. Eur. J. Cell Biol. 90, 787–796.

14. Furuse, M., and Tsukita, S. (2006). Claudins in occluding junctions of humans and flies. Trends Cell Biol. 16, 181–188.

15. Tepass, U., and Hartenstein, V. (1994). The development of cellular junctions in the Drosophila embryo. Dev. Biol. 161, 563–596.

16. Lane, N.J., and Skaer, H. (1980). Intercellular junctions in insect tissues, pp. 35–213.

17. Resnik-Docampo, M., Sauer, V., Schinaman, J.M., Clark, R.I., Walker, D.W., and Jones, D.L. (2018). Keeping it tight: the relationship between bacterial dysbiosis, septate junctions, and the intestinal barrier in Drosophila. Fly 12, 34–40.

18. Apidianakis, Y., and Rahme, L.G. (2011). Drosophila melanogaster as a model for human intestinal infection and pathology. Dis. Model. Mech. 4, 21–30.

19. Ohlstein, B., and Spradling, A. (2007). Multipotent Drosophila intestinal stem cells specify daughter cell fates by differential Notch signaling. Science 315, 988–992.

20. Micchelli, C.A., and Perrimon, N. (2006). Evidence that stem cells reside in the adult Drosophila midgut epithelium. Nature 439, 475–479.

21. Reiff, T., Antonello, Z.A., Ballesta-Illán, E., Mira, L., Sala, S., Navarro, M., Martinez, L.M., and Dominguez, M. (2019). Notch and EGFR regulate apoptosis in progenitor cells to ensure gut homeostasis in Drosophila. EMBO J. 38, e101346.

22. Korzelius, J., Azami, S., Ronnen-Oron, T., Koch, P., Baldauf, M., Meier, E., Rodriguez-Fernandez, I.A., Groth, M., Sousa-Victor, P., and Jasper, H. (2019). The WT1-like transcription factor Klumpfuss maintains lineage commitment of enterocyte progenitors in the Drosophila intestine. Nat. Commun. 10, 4123.

23. Li, H., and Jasper, H. (2016). Gastrointestinal stem cells in health and disease: from flies to humans. Dis. Model. Mech. 9, 487–499.

24. Jiang, H., Patel, P.H., Kohlmaier, A., Grenley, M.O., McEwen, D.G., and Edgar, B.A. (2009). Cytokine/Jak/Stat signaling mediates regeneration and homeostasis in the Drosophila midgut. Cell 137, 1343–1355.

25. Choi, Y.J., Hwang, M.S., Park, J.S., Bae, S.K., Kim, Y.S., and Yoo, M.A. (2008). Age-related upregulation of Drosophila caudal gene via NF-kappaB in the adult posterior midgut. Biochim. Biophys. Acta 1780, 1093–1100.

26. Park, J.S., Kim, Y.S., and Yoo, M.A. (2009). The role of p38b MAPK in age-related modulation of intestinal stem cell proliferation and differentiation in Drosophila. Aging 1, 637–651.

27. Byri, S., Misra, T., Syed, Z.A., Bätz, T., Shah, J., Boril, L., Glashauser, J., Aegerter-Wilmsen, T., Matzat, T., Moussian, B., et al. (2015). The triple-repeat protein anakonda controls epithelial tricellular junction formation in Drosophila. Dev. Cell 33, 535–548.

28. Hildebrandt, A., Pflanz, R., Behr, M., Tarp, T., Riedel, D., and Schuh, R. (2015). Bark beetle controls epithelial morphogenesis by septate junction maturation in Drosophila. Dev. Biol. 400, 237–247.

29. Sarov, M., Barz, C., Jambor, H., Hein, M.Y., Schmied, C., Suchold, D., Stender, B., Janosch, S., Kj, V.V., Krishnan, R.T., et al. (2016). A genome-wide resource for the analysis of protein localisation in Drosophila. Elife 5, e12068.

30. Brand, A.H., and Perrimon, N. (1993). Targeted gene expression as a means of altering cell fates and generating dominant phenotypes. Development 118, 401–415.

31. Osterwalder, T., Yoon, K.S., White, B.H., and Keshishian, H. (2001). A conditional tissue-specific transgene expression system using inducible GAL4. Proc. Natl. Acad. Sci. USA 98, 12596–12601.

32. Esmangart de Bournonville, T., and le Borgne, R. (2020). Interplay between anakonda, Gliotactin, and M6 for tricellular junction assembly and anchoring of septate junctions in Drosophila epithelium. Curr. Biol. 30, 4245–4253.

33. Rera, M., Bahadorani, S., Cho, J., Koehler, C.L., Ulgherait, M., Hur, J.H., Ansari, W.S., Lo, T., Jones, D.L., and Walker, D.W. (2011). Modulation of longevity and tissue homeostasis by the Drosophila PGC-1 homolog. Cell Metabol. 14, 623–634.

34. Dutta, D., Dobson, A.J., Houtz, P.L., Gläßer, C., Revah, J., Korzelius, J., Patel, P.H., Edgar, B.A., and Buchon, N. (2015). Regional cell-specific transcriptome mapping reveals regulatory complexity in the adult Drosophila midgut. Cell Rep. 12, 346–358.

35. Hung, R.J., Li, J.S.S., Liu, Y., and Perrimon, N. (2021). Defining cell types and lineage in the Drosophila midgut using single cell transcriptomics. Curr. Opin. Insect Sci. 47, 12–17.

36. Antonello, Z.A., Reiff, T., Ballesta-Illan, E., and Dominguez, M. (2015). Robust intestinal homeostasis relies on cellular plasticity in enteroblasts mediated by miR-8–Escargot switch. EMBO J. 34, 2025–2041.

37. Ohlstein, B., and Spradling, A. (2005). The adult Drosophila posterior midgut is maintained by pluripotent stem cells. Nature 439, 470–474.

38. Furriols, M., and Bray, S. (2000). Dissecting the mechanisms of suppressor of hairless function. Dev. Biol. 227, 520–532.

39. Biteau, B., Karpac, J., Supoyo, S., DeGennaro, M., Lehmann, R., and Jasper, H. (2010). Lifespan extension by preserving proliferative homeostasis in Drosophila. PLoS Genet. 6, e1001159.

40. Zhai, Z., Kondo, S., Ha, N., Boquete, J.P., Brunner, M., Ueda, R., and Lemaitre, B. (2015). Accumulation of differentiating intestinal stem cell progenies drives tumorigenesis. Nat. Commun. 6, 10219–10313.

41. Chen, J., and St Johnston, D. (2022). De novo apical domain formation inside the Drosophila adult midgut epithelium. Elife 11, e76366. https://doi.org/10.7554/eLife.76366.

42. Wittek, A., Hollmann, M., Schleutker, R., and Luschnig, S. (2020). The transmembrane proteins M6 and anakonda cooperate to initiate tricellular junction assembly in epithelia of Drosophila. Curr. Biol. 30, 4254–4262.

STAR★METHODS

KEY RESOURCES TABLE

REAGENT or RESOURCE	SOURCE	IDENTIFIER
Antibodies		
Mouse monoclonal anti-Armadillo	DSHB	Cat #N2 7A1, RRID:AB_528089
Guinea pig polyclonal anti-Bark	Laboratory of Reinhard Schuh (MPI for Multidisciplinary Sciences)	N/A
Mouse monoclonal anti-Dlg1	DSHB	Cat #4F3, RRID:AB_528203
Chicken polyclonal anti-GFP	Aves Labs	Cat #GFP-1010, RRID:AB_2307313
Chicken polyclonal anti-GFP	Abcam	Cat #ab13970, RRID:AB_300798
Rabbit polyclonal anti-GFP	Molecular Probes	Cat #A-11122, RRID:AB_221569
Rabbit polyclonal anti-pHH3	Millipore	Cat #06-570, RRID:AB_310177
Mouse monoclonal anti-Pros	DSHB	Cat #MR1A, RRID:AB_528440
Goat anti-chicken Alexa488	Invitrogen	Cat #A-11039, RRID:AB_142924
Goat anti-guinea pig Alexa568	Invitrogen	Cat #A-11075, RRID:AB_141954
Goat Anti-mouse Alexa568	Invitrogen	Cat #A-11004, RRID:AB_2534072
Goat anti-mouse Alexa647	Invitrogen	Cat #A-21235, RRID:AB_2535804
Donkey anti-rabbit Alexa647	Invitrogen	Cat #A-31573, RRID:AB_2536183
Chemicals, peptides, and recombinant proteins		
RU-486	Sigma	Cat #M8046
FD&C Blue Dye no. 1	Spectrum Chemical	Cat #FD110
Erioglaucine Disodium Salt (E133)	BLD Pharmatech Ltd., Shanghai, China	Cat #3844-45-9
Experimental models: Organisms/strains		
D. melanogaster: tub-GAL80^{ts}	Bloomington *Drosophila* Stock Center	BDSC: 7017
D. melanogaster: Gli::GFP	Kyoto Stock Center	DGRC #115-332
D. melanogaster: w^{1118}	Laboratory of D. Walker (U. of California-Los Angeles)	N/A
D. melanogaster: Su(H)lacZ; esg:GFP, 5966GAL4^{GS}	Laboratory of B. Ohlstein (UT Southwestern)	N/A
D. melanogaster: 5966-GAL4^{GS}	Laboratory of H. Jasper (Buck Institute)	N/A
D. melanogaster: Myo1A-GAL4	Laboratory of H. Jasper (Buck Institute)	N/A
D. melanogaster: P{bark.Ty1-Tev-SGFP-FLAG}	Laboratory of S. Luschnig (U. of Münster)	N/A
D. melanogaster: yw hsflp; Sco/Cyo Dfd-GMR nuGFP; UAS-bark attP2y (L057)	Laboratory of S. Luschnig (U. of Münster)	N/A
D. melanogaster: Gbe+Su(H)GFP	Laboratory of T. Klein (U. of Düsseldorf)	N/A
D. melanogaster: w; esg-GAL4,UAS-CD8::GFP; UAS-H2B::RFP, tub-GAL80ts	Antonello et al. 2015	N/A
D. melanogaster: w; UAS-CD8::GFP, tub-GAL80^{ts}; klu-GAL4, UAS-H2B::RFP	Reiff at al. 2019	N/A
D. melanogaster: w; UAS-CD8::GFP, tub-GAL80^{ts}; klu-GAL4, UAS-H2B::RFP	Laboratory of T. Reiff (U. of Düsseldorf)	N/A
D. melanogaster: w; UAS-CD8::RFP, tub-GAL80^{ts}; klu-GAL4, UAS-H2B::RFP	Laboratory of T. Reiff (U. of Düsseldorf)	N/A
D. melanogaster: esg-GAL4; UAS-H2B::RFP	Laboratory of Tobias Reiff (U. of Düsseldorf)	N/A
D. melanogaster: esg-GFP; UAS-H2B::RFP	Laboratory of Tobias Reiff (U. of Düsseldorf)	N/A
D. melanogaster: UAS-bark-RNAi^{GD}	Vienna *Drosophila* Resource Center	v52608

(Continued on next page)

Continued

REAGENT or RESOURCE	SOURCE	IDENTIFIER
D. melanogaster: UAS-bark-RNAi[KK]	Vienna *Drosophila* Resource Center	v107348
D. melanogaster: UAS-Gli RNAi	Vienna *Drosophila* Resource Center	V37115
Software and algorithms		
Prism v8.0.2	Graphpad	N/A
Illustrator CC 2020	Adobe	N/A
ImageJ 1.51n	Wayne Rasband, NIH	https://imagej.nih.gov/ij
ZEN Blue v.3.3	Zeiss	N/A
ZEN Black v.2.0	Zeiss	N/A
Canvas X-Pro	Canvas X-Pro 2019	N/A

RESOURCE AVAILABILITY

Lead contact

Further information and requests for resources and reagents should be directed to and will be fulfilled by the lead contact, Leanne Jones (leanne.jones@ucsf.edu).

Materials availability

This study did not generate new unique reagents.

Data and code availability

- All data reported in this paper is available from the lead contact upon request.

- This paper does not report original code.

- Any additional information required to reanalyze the data reported in this paper is available from the lead contact upon request.

EXPERIMENTAL MODEL AND STUDY PARTICIPANT DETAILS

Set 1: Fig. 1C, Figs. 5-6, Fig. EV2H-K, Figs. EV3-EV4.

Set 2: Fig. 1A-B, Figs. 2–4, Fig. EV1, Fig. EV2A-G.

Set 1

Fly food contained 7.12% corn meal, 4.5% malt extract, 4% sugar beet syrup, 1.68% dried yeast, 0.95% soy flour, 0.5% agarose, 0.45% propionic acid, and 0.15% NIPAGIN powder (antimycotic agent). $GAL80^{ts}$ flies were kept at 18°C (permissive temperature) until shifted to 29°. Otherwise, flies and crosses were kept at 25°C. All analyses were performed on 3-7 day old (do) mated females that were shifted to 29°C for 7 days for tracing. A maximum of 20 flies (females and males) were housed in one fly vial.

Set 2

Flies were cultured in vials containing standard cornmeal medium (1.1% agar, 2.9% baker's yeast, 9.2% maltose, and 7.1% cornmeal; all concentrations given in wt/vol). Propionic acid (0.5%) and TegoSept (methylparaben, Sigma, 0.16%) were added to adjust pH and prevent fungal growth, respectively. No more than 30 flies were housed per vial. All experiments were conducted at 25°C. Newly eclosed adults were kept for an additional 1–2 days before inducing transcription activation by placement on food containing the steroid hormone mifepristone (RU-486, Sigma) in a 25 μg/ml concentration and flipped every 2 days thereafter. All analyses for these studies were performed on female flies, as age-related gut pathology has been well established in females.[3,7]

METHOD DETAILS

Immunohistochemistry

Set 1

Dissected guts were fixed in 4% PFA in 1XPBS for 45 min. After fixation the guts were washed with 1XPBS for 10 min and stained with primary antibodies, diluted in 0.5% PBT (0.5% Triton (Sigma-Aldrich) in 1XPBS) + 5% normal goat serum (Thermo Fisher Scientific, Berman, Germany). Primary antibody staining was performed at 4°C overnight on an orbital shaker. Primary antibodies used were mouse anti-Dlg1 (DSHB, 1:250), chicken anti-GFP (Abcam, 1:250), rabbit anti-pHH3 (Millipore, 1:200), and mouse anti-Pros (DSHB, 1:250). On the next day, guts were washed with 1XPBS for 10 min and incubated with secondary antibodies and DAPI (1:1000; 100 μg/mL stock solution in 0.18 M Tris pH 7.4; DAPI No. 18860, Serva, Heidelberg) for at least 3 h at RT. After washing with 1XPBS for 10 min the stained guts were mounted in Fluoromount-G Mounting Medium (Electron Microscopy Sciences). Stained posterior midguts were imaged in the R5 region using an LSM 710 confocal microscope (Carl Zeiss) with 'Plan-Apochromat 20 × /0.8 M27' and 'C-Apochromat 40 × /1.20 W Corr M27' objectives. Image resolution was set to at least 2048 × 2048 pixels. Focal planes were combined into Z-stacks and images were then processed by Fiji software. Final images were assembled using Canvas X-Pro.

Set 2

All images were taken in the P3–P4 regions of the *Drosophila* PMG, located by centering the pyloric ring in a ×40 field of view (fov) and moving 1–2 fov toward the anterior. PMGs were dissected into ice-cold PBS/4% formaldehyde and incubated for 1 h in fixative at room temperature. Samples were then washed three times, for 10 min each, in PBT (PBS containing 0.5% Triton X-100), 10 min in Na-deoxycholate (0.3%) in PBT (PBS with 0.3% Triton X-100), and incubated in block (PBT-0.5% bovine serum albumin) for 30 min at room temperature. Samples were immunostained with primary antibodies overnight at 4°C. Primary antibodies used were mouse anti-Armadillo (DSHB, 1:20), guinea pig anti-Bark (gift from Reinhard Schuh, 1:1000), mouse anti-Dlg1 (DSHB, 1:250), chicken anti-GFP (Aves Labs, 1:500), chicken anti-GFP (Abcam, 1:200), rabbit anti-GFP (Molecular Probes, 1:3000), and rabbit anti-pHH3 (Millipore, 1:200). Samples were washed 3 × 10 min at room temperature in PBT (PBS containing 0.5% Triton X-100), incubated with secondary antibodies (1:500, Invitrogen) at room temperature for 2 h, washed 3 × 10 min with PBT and mounted in Vecta-Shield/DAPI (Vector Laboratories, H-1200). Images were acquired on a Zeiss LSM780 or LSM880 inverted confocal microscope (UCLA MCDB/BSCRC Microscopy Core), and on a Zeiss Axio Observer Z1 with Apotome 2 using the ZEN Black v.2.0 (Zeiss) software. Images were processed with Fiji/ImageJ and Zen Blue v.3.3 (Zeiss) software. Final figures were assembled using Adobe Illustrator.

Smurf assay

Figure 4

Smurf assay: A stock solution of Erioglaucine Disodium Salt (E133) (BLD Pharmatech Ltd., Shanghai, China) of concentration 320 g/l was prepared. To prepare the food for the Smurf assay, 300 μl of the stock solution was mixed with 4 ml of standard food medium. Flies were checked daily for loss of barrier function.

Figure 5

Flies were maintained on standard medium prepared with FD&C Blue Dye no. 1, added at a concentration of 2.5% (wt/vol). Loss of intestinal barrier function was determined ("Smurf" status) when dye was clearly observed outside the digestive tract.[33] Flies were checked three times weekly for loss of barrier function and/or death.

Survival analysis

Flies were kept at 18°C and 3-5 days old flies were then shifted to 29°C. Not more than 10 flies (1:1 ratio of females:males) were kept per vial and flipped every other day to avoid bacterial contamination in the food. Flies were checked daily to record death events. At least 80 flies were assessed per genotype. Survival curves were plotted using Prism GraphPad software.

QUANTIFICATION AND STATISTICAL ANALYSIS

Quantification of proliferation

Quantification of mitotic events, as measured by pHH3$^+$ cells per gut, was performed by acquiring 4 independent images at 40X magnification per gut in the P3-P4 region.

Quantification of nuclear size and fluorescence intensity

Nuclear size measurements were performed in Fiji by outlining the nucleus manually and measuring the area. Mean intensities of the manually selected nuclear area were measured using Fiji by manually selecting the area of interest.

Quantification of cell counts

GFP positive progenitor cells and RFP positive differentiated cells (EC and/or EE) of esg^{ReDDM},[36] klu^{ReDDM}, and $Myo\text{-}GAL4^{ts}$ were counted manually.

Quantification of tSJ and cytoplasmic fluorescence intensity

Quantification of antibody fluorescence at the tSJ and cytoplasm was performed with the ZEN Blue software. Images were acquired on a Zeiss LSM880 inverted confocal microscope equipped with AiryScan at 100X. Full z-stacks were used, and anti-Armadillo staining was used to mark membranes. 3 cells were measured per PMG. Each clearly visible tSJ in the cell was measured. 6 measurements of the cytoplasm were taken in each cell.

Quantification of BCJ fluorescence intensity

Figure 3, S4

Quantification of antibody fluorescence at the bSJ was performed with the ZEN Blue software. Images were acquired on a Zeiss LSM880 inverted confocal microscope equipped with AiryScan at 100X. Full z-stacks were used, and anti-Armadillo staining was used to mark membranes. 3 cells were measured per PMG. 6 measurements were taken of the bicellular junction in each cell.

Figure 6

Images were taken in directly adjacent fields of view on each side of the gut in the R5 region. Quantification of progenitor cell number and epithelial renewal were performed manually. Cell size and fluorescence intensity measurements were performed on Fiji (ImageJ 1.51 n, Wayne Rasband, National Institutes of Health, USA) by outlining the cell of interest.

Statistics

GraphPad Prism 8.0.2 was used to run statistical analysis and create graphs of quantifications. For single comparisons, data sets were analyzed by two-sided unpaired t-test or Mann-Whitney test. Multiple comparisons were analyzed by one-way ANOVA or Kruskal-Wallis tests. For survival analyses, Mantel-Cox log-rank test was performed. Significant differences are displayed as * for $P \leq 0.05$, ** for $P \leq 0.01$, *** for $P \leq 0.001$ and **** for $P \leq 0.0001$. Experiments were repeated at least twice. No statistical method was used to predetermine sample size. Experiments were not randomized, and researchers were not blinded to allocation during experiments or outcome assessment. Statistical tests and significance used in each figure can also be found in figure legends.